

Nanometer-Scale Investigation of Metal-SiC Interfaces using Ballistic Electron Emission Microscopy

H.-J. Im,¹ B. Kaczer,¹ J. P. Pelz,¹

S. Limpijumnong,² W. R. L. Lambrecht,²

and

W. J. Choyke³

¹ *Department of Physics, The Ohio State University, Columbus, OH 43210*

² *Department of Physics, Case Western Reserve University, Cleveland, OH 44106*

³ *Department of Physics and Astronomy, University of Pittsburgh, Pittsburgh, PA 15260*

(Author correspondence: e-mail: hjim@mps.ohio-state.edu, fax: ++1 (614) 292-7557)

Abstract: We report ballistic-electron emission microscopy (BEEM) investigation of Pd, Pt Schottky contacts on 6H-, 4H-SiC and Pd/15R-SiC. Measured Schottky barrier heights (SBH's) of 6H- and 4H-SiC samples appear spatially uniform up to the fitting error due to noise (0.03—0.04 eV and 0.1—0.2 eV for 6H- and 4H-SiC, respectively). In 4H-SiC, we observed an additional conduction band minimum (CBM) ~0.14 eV above the lowest CBM, which provide direct experimental verification of band theoretical calculation results. Additionally, we sometimes observed *enhancement* in ballistic transmittance over regions intentionally stressed by hot electron injection using BEEM. We also report recent results on Pd/15R-SiC sample indicating a higher CBM ~0.5 eV above the lowest CBM. In Pd/15R-SiC, interesting large variations in BEEM spectra at different locations were observed, possibly suggesting an inhomogeneous metal/semiconductor interface.

I. Introduction

In recent years, there has been a great deal of interest in a variety of “wide-bandgap” materials for a number of advanced electronic and optical applications.^{1,2} For example, SiC has a moderately wide bandgap (2.4—3.3 eV, depending on polytypes), excellent thermal conductivity and high breakdown electric field, and hence is a leading material for many high power, high temperature, high frequency, and radiation-resistant applications. The III-nitrides (including InN, GaN, and AlN) can be grown with direct bandgaps ranging from 1.9 eV to 6.2 eV, making them ideal candidates for a variety of optical detection and emission applications at wavelengths spanning red to ultra-violet. However, the quality and electronic properties of these materials (especially at the critical *interfaces* of these materials) are still far from well understood or optimized, and a great deal of material improvement and characterization must still be done before they can be reliably “engineered” for specific applications. In particular, little is yet known about possible *microscopic variations* of interfacial properties, which could seriously affect electronic and optical properties of devices made from these materials, particularly as devices are scaled to very small lateral dimensions. Several authors have suggested that significant spatial variations in Schottky barrier height (SBH) may exist for metal contacts on the *6H* polytype of SiC, which might explain observed discrepancies in the spatially-averaged SBH measured by different macroscopic techniques.³⁻⁵ Spatial variations in interfacial properties are expected to be even more severe on the III-nitrides, since these materials are currently grown with a high density of dislocation, grain boundaries, and other internal microstructure. To date, however, few direct *microscopic* studies of interfacial properties have been done on these technologically important wide-bandgap materials.

Here we report microscopic interface measurements using ballistic-electron emission

microscopy (BEEM)⁶ of Schottky contacts on the *6H*, *4H*, and *15R* polytypes of SiC. We find that BEEM is a powerful and versatile technique for studying buried interfaces on wide-bandgap materials⁷ which can provide direct information about local interface electronic properties, local hot-electron degradation properties, and interfacial band structure which are not readily available by other techniques. Section II briefly describes metal/SiC sample preparation and computational methods for electronic band structures, while Section III describes the BEEM technique and its implementation for studies of metal/SiC interfaces. Section IV and V review our initial BEEM measurements of the spatial uniformity, interfacial conduction band structure, and hot-electron stressing effects of the *6H*- and *4H*-SiC polytypes.^{8,9} Section VI focuses on our recent BEEM measurements of the conduction band structure of the *15R*-SiC polytype, where we observe strong experimental evidence of a high-lying conduction band minimum (CBM) located about 0.5 eV above the lowest CBM. The energy of this higher CBM is in agreement with our first-principle band structure calculations. However, we also observe large spatial variations in the BEEM spectra on our *15R*-SiC sample, possibly indicating significant microscopic spatial variations in the interfacial band structure of this sample.

II. Sample preparation and computational methods

The SiC samples used in these studies consisted of ~ 2 μm -thick lightly *n*-type SiC ($N_D \sim 3 \times 10^{16} \text{ cm}^{-3}$, nitrogen doped) epitaxially grown using chemical vapor deposition (CVD) on *n*-type ($N_D \sim 5 \times 10^{18} \text{ cm}^{-3}$) *6H*-, *4H*-, or *15R*-SiC substrates. The samples were cleaned *ex situ* by several cycles of a sacrificial surface oxidation (using ultra-violet ozone) followed by an HF etch.⁸ The samples were introduced into an ultra-high vacuum (UHV) chamber (base pressure $\sim 10^{-10}$ Torr),

out-gassed for several hours at ~ 230 °C, and then Schottky contacts were formed by depositing Pd or Pt film (typically 6-10 nm thick, by e-gun evaporation) through a shadow mask producing an array of 0.5 mm diameter circular dots. The samples were then transported in UHV into the STM/BEEM chamber, where the dots were individually contacted with a thin Au wire. We first measured conventional I - V curves on each metal/SiC contact thus formed, and the dots exhibiting the best ideality factor¹⁰ (usually in the range 1.05—1.09) were then investigated using BEEM measurements. Metal depositions and all the measurements were performed at room temperature.

The 15*R*-SiC sample used in these measurements requires a special note. When the SiC substrate material was produced, a region of 15*R*-SiC nucleated and grew side-by-side with a 6*H*-SiC region, and both polytypes were present (in separate regions) in the 5×5 mm² substrate onto which the epitaxial SiC film was grown. It turned out that some of the deposited Pd metal dots were located on the 15*R* region, while some were on the 6*H* region. Hence on this sample, Schottky contact to both polytypes could be measured on the same substrate wafer.

We performed full-potential linear muffin-tin orbital (LMTO) band structure calculations¹¹ of the SiC polytypes under consideration using the local density functional approximation (LDA). Details of our computational approach for SiC and a more complete discussion of the band structure results is given elsewhere.¹⁵ To obtain the densities of states with high accuracy revealing the van Hove type singularities, the bands were calculated on a fine mesh of $n \times n \times n$ points (with n typically about 15—20) in the reciprocal space (k -space) region containing the relevant bands near the CBM and linear interpolation of the bands was used between those points as in the linear tetrahedron method.

III. Ballistic-Electron Emission Microscopy (BEEM)

BEEM is an extension of scanning tunneling microscopy (STM), which can be used to probe *local* electronic properties of buried metal/semiconductor (MS) interfaces with nanometer-scale spatial resolution and high energy resolution.⁶ The basic idea of BEEM is illustrated in Fig. 1, which shows the experimental setup, and corresponding energy-level diagram. The sample consists of a thin metal film on a substrate such that there is an electronic energy barrier (e.g. a Schottky barrier) separating the interfacial CBM in the substrate from the Fermi level electrons in the metal film. For BEEM, it is useful to think of the STM tip as an adjustable local hot electron injector, with the hot electron peak energy in the metal film controlled by the applied tip bias V_T , the hot electron current controlled by the tip-sample distance d , and the injection point controlled by the lateral position of the tip. Provided that the metal film is thin enough compared with the hot electron mean free path in the metal over-layer, a fraction of the injected hot electrons can cross the metal film elastically, enter the substrate conduction band (if injected with sufficient energy to get over the barrier), and be measured as the substrate or “collector” current I_c .

In one mode of using BEEM, the *local* SBH qF_B can be directly determined by measuring BEEM I_c - V_T curves (also called BEEM spectra) and evaluating the threshold voltage V_{th} above which non-zero BEEM current is observed. This mode of using BEEM is sometimes referred to as ballistic-electron emission spectroscopy (BEES). Figure 2 shows an example of such BEEM I_c - V_T curves on metal/6H-SiC contacts made with Pd and Pt, where each set of data represents an average of 125—150 individual BEEM I_c - V_T curves measured at different sample locations. The data near threshold were then fit using the Bell-Kaiser (BK) model for BEEM spectrum,⁶ shown as the solid curves. The BK theory assumes, among others, parabolic conduction band of semiconductor and

conservation of energy and transverse momentum at interfaces. The theory neglects, however, possible effects of non-parabolic semiconductor conduction band structure, metal over-layer band structure, and quantum mechanical transport effects at the MS interface, and hence is expected to be less accurate at voltages well above threshold. Details of the procedures and parameters used for these fits are described elsewhere.⁹ The arrows indicate the threshold voltage for each curve as determined by the fit, which indicate SBH's of 1.27 ± 0.02 eV and 1.34 ± 0.02 eV for Pd and Pt, respectively.

It has also been shown that BEEM can detect higher energy CBM's in the semiconductor band structure.⁶ When the tip voltage V_T reaches a value such that injected electron have sufficient energy to enter a higher energy CBM (illustrated by the curve marked as CBM₂ in Fig. 1(b)), there will be an onset of *additional* BEEM current I_c , which generally shows up as a local increase in the slope of the derivative of BEEM I_c - V_T curve. We will return to this point later.

BEEM was initially applied to metal contacts on Si and GaAs. Recently, BEEM has been applied to several wide-bandgap materials, including SiC,^{8,9} GaN,⁷ CaF₂,¹² and SiO₂.^{13,14} In some ways, BEEM works *better* on wide-bandgap materials, since the energy barriers tend to be larger with these materials, causing background current and current noise to be much smaller than for narrower bandgap materials. Because of these large barriers, it is also possible to make BEEM measurements in the presence of a substantial reverse bias across the MS interface without substantially increasing the current noise. This is illustrated in Fig. 3, which shows the measured barrier height *vs.* reverse sample bias V_b on a 10 nm-Pd/6H-SiC contact. For each data points, 25 individual BEEM I_c - V_T curves were averaged, and then fit with the BK model to determine the threshold voltage. The systematic decrease in the barrier height with increasing V_b is due to the well known “image force lowering” effect, as illustrated in the inset. The solid curve is a fit to the data

using the image force model,¹⁰ and from this fit it is possible to determine the “flat band” barrier height to within a few meV. In general, making BEEM measurements under large interface electric fields is potentially useful for characterizing trapped charge near the interface (as we did with metal/SiO₂ interfaces),¹³ and for studies of hot-electron stressing effects under large electric field conditions. In what follows in this paper, however, V_b was kept at zero when data were taken.

IV. Spatial homogeneity of the Schottky barrier

In several previous studies of SBH's on 6H-SiC using conventional macroscopic techniques,³⁻⁵ it was observed that some methods of measuring SBH's (such as current-voltage (I - V) curves or X-ray photoelectron spectroscopy (XPS)) indicated consistently lower SBH's than other methods (such as capacitance-voltage (C - V) curves). It was suggested that this systematic discrepancy (as well as other “anomalous” behavior of a Schottky contact) may be explained by assuming local spatial variation of SBH at the MS interface, since such spatial variation would affect the average SBH determined by each method in different ways. In particular, conventional I - V curves should be more sensitive to small regions with low barrier height than C - V curves, resulting in a lower average SBH.

We have used the nanometer-scale spatial resolution inherent to BEEM to investigate possible SBH variations on 6H-SiC. This was done by fitting *individual* BEEM spectrum taken at different locations, then looking for spatial variations in the extracted SBH's. Statistical analysis on the obtained SBH distribution shows a narrow peak with a one- σ spread of ~ 0.03 eV and ~ 0.04 eV for Pd/ and Pt/6H-SiC samples, respectively.⁸ We note the signal-to-noise ratio for individual BEEM I_c - V_T curves is worse than for averaged BEEM I_c - V_T curves (such as that shown in Fig. 2),

resulting in larger fitting errors for the extracted SBH's of about 0.03—0.04 eV. Since this is roughly the same magnitude as the measured variation in SBH, we conclude that any “real” SBH variations of our 6H-SiC samples must be smaller than ~ 0.04 eV. This small variation in measured SBH suggests that our 6H-SiC Schottky contacts had rather uniform interfacial energy barriers. We note that our own conventional I - V measurements of our Pd/ and Pt/6H-SiC samples yielded SBH's of 1.27 eV and 1.26 eV, respectively, which agree fairly well with the SBH's determined by BEEM. This further supports our conclusion that these 6H-SiC samples had fairly uniform SBH. Microscopic measurements such as these should be very useful in future studies of Schottky contacts on SiC in which spatial inhomogeneities are suspected.

V. Electronic band structures and stability of Schottky contacts

The Schottky barrier represents the energy of the lowest CBM at MS interfaces. Besides determining the local SBH, BEEM spectra also contain important information about the semiconductor band structure at higher energy.⁶ As discussed in Section III, a higher-energy CBM should produce a recognizable feature in BEEM I_c - V_T curves at a tip voltage corresponding to the energy of the CBM. In the BEEM I_c - V_T curves for 6H-SiC shown in Fig. 2, we do not see evidence of any additional CBM's close to the lowest CBM. However, we have also made BEEM measurements of Pd and Pt contacts on 4H-SiC, and in this case we do observe evidence of an additional CBM located ~ 0.14 eV above the lowest CBM.^{8,9} Figure 4 shows averaged BEEM I_c - V_T data from Pd/ and Pt/4H-SiC samples, and the inset shows the derivative spectrum dI_c/dV_T vs. V_T of the Pd/4H-SiC sample. We see from the inset a distinct increase in slope at ~ 0.14 V above the lowest threshold voltage, indicating the existence of an additional CBM. The solid curves in Fig. 4

show fits to the data using the BK model, where now we allow two independent thresholds as indicated by the arrows. For both the Pd/ and Pt/4H-SiC samples, we could only get reasonable fits to the data if we allowed two thresholds.⁹

The measured energy separation of ~ 0.14 eV between the second CBM and the lowest CBM is in good agreement with band structure calculations for 4H-SiC made by ourselves and others which indicate an additional CBM about 0.11—0.13 eV above the lowest CBM.^{9,15} This is illustrated in Fig. 5, which shows calculated total conduction band density of states (DOS) vs. energy of 6H- and 4H-SiC, measured relative to the CBM. Although the derivative BEEM spectrum does not directly map DOS of the semiconductor, it is expected that each additional CBM should produce an abrupt increase in DOS, as well as additional onset in BEEM I_c - V_T curves at the corresponding voltage. We see from Fig. 5 that the DOS for 6H-SiC does not show any distinct increases close to the CBM, while the 4H-SiC DOS does show an abrupt increase near ~ 0.12 eV, which is due to an additional CBM. To the best of our knowledge, our BEEM measurements^{8,9} provide the first quantitative experimental determination of the energy of the second CBM.

Here, we note a few specific points about the calculated band structures. In 6H-SiC, the saddle point type discontinuity in slope in the DOS of the first band coincides with the minimum of the second band and occurs at the L -point in the Brillouin zone (BZ).^{9,15} When the second band is folded out in the second BZ, however, there is no discontinuity in slope of $E(k)$. This is because the bands are degenerate at L due to the six-fold screw axis symmetry in the hexagonal polytypes. In this sense one can think of these two bands as a single monotonically increasing band in an extended zone scheme. Correspondingly, there is *no* discontinuity and no sharp increase in DOS vs. E associated with this point in k -space. In contrast, in 4H-SiC, the second band decreases from L to M and leads to a well-defined separate minimum at M with a well-defined sharp increase in DOS.

We now note several other interesting things about the BEEM spectra for $6H$ - and $4H$ -SiC. First, the determined SBH's (the lowest threshold) of Pd/ and Pt/ $4H$ -SiC are 1.54 ± 0.03 eV and 1.58 ± 0.03 eV, respectively. It is interesting to note that the SBH differences between $4H$ - and $6H$ -SiC are very close to the band-gap difference between the two polytypes, 0.24 eV. Second, we note that Pt contacts show slightly larger SBH's than Pd contacts which probably results from the slightly larger work function of Pt.¹⁶ Finally, we notice from Fig. 2 and Fig. 4 that the BEEM spectra for the contacts made with Pd (on both $6H$ -SiC and $4H$ -SiC) tend to roll over slightly at higher tip voltage (*i.e.*, are concave down), while the BEEM spectra for contacts made with Pt tend to curve up slightly (concave up) at higher tip voltage. This systematic difference in shape may reflect differences between the *metal* structure of Pd and Pt, which could affect the shape of BEEM I_c - V_T curves.¹⁷

We also used BEEM to perform microscopic investigations of hot-electron-induced interface modification. This is potentially important because SiC is the most promising material for high-voltage, high-current device applications. In the experiment, relatively long (40 min) stressing scans were performed over a microscopically small (50×50 nm²) region by injecting high kinetic energy (10 eV above E_F) electrons in a Pt/ $4H$ -SiC sample. We estimate that at least ~ 5 pA of the hot electron current crosses the metal film without scattering, and are concentrated in a region less than ~ 5 nm across.⁶ This corresponds to a hot-electron exposure of at least $\sim 6 \times 10^4$ C cm⁻². Most of the time, we found that the Schottky contact was not noticeably affected by this level of hot-electron stressing. Occasionally, however, we observed a small *enhanced* ballistic electron transmittance across the MS interface (but little change in barrier height) over the intentionally stressed region.⁸ This is illustrated in Fig. 6, which shows “before” and “after” images of the top metal topography (left panels) and the corresponding BEEM images (right panels), where the BEEM image is simply a

plot of I_c vs. position with the tip voltage held at a constant value above threshold. Most of the splotchy contrast seen in the BEEM images is due to variations in the thickness of the metal overlayer, and is seen to be very nearly the same after stressing as before. However, the stressed region shows a small but systematic increase in I_c as compared with the non-stressed regions. We note that Hallen and co-workers have reported similar enhanced ballistic transmittance on stressed Au/Si Schottky contacts, which was attributed to thinning of an interfacial layer.¹⁸ A similar mechanism may be responsible for what we occasionally observed on SiC. We note here that our SiC surfaces were chemically cleaned *ex situ* and transferred through air to the UHV system, and hence it is quite possible that they could have formed a thin oxide layer prior to metal deposition. In future experiments we will clean the SiC surface in UHV prior to metal deposition, and hence will be able to investigate how interface preparation affects the hot-electron stressing behavior of the metal/SiC interface.

VI. Results from 15R-SiC

More recently, we have performed similar BEEM investigations on Pd contacts on the 15R-SiC polytype. In this case, we observed a strong indication that there is another CBM at about 0.5 eV higher than the lowest CBM. Figure 7 shows averaged BEEM spectra measured at a certain location on the Pd/15R-SiC sample, and the inset shows the derivative BEEM. We see from the inset that there is a clear increase in slope at about 0.50—0.55 V higher than the threshold voltage of $V_{th} \cong 1.22$ V, suggesting the existence of an additional CBM ~ 0.5 eV above the lowest CBM. Using first principles band structure calculations, we indeed find a CBM in 15R-SiC about 0.50 eV above the lowest CBM. Figure 8(a) shows the calculated two lowest lying conduction bands in 15R-SiC.

The lowest CBM is located at the X -point of the $15R$ -SiC BZ, while the minimum of the second conduction band is located at the L -point, at an energy about 0.50 eV above the lowest CBM. This calculated separation between the two lowest CBM's agrees very well with the BEEM data. Figure 8(b) shows calculated total DOS for $15R$ -SiC conduction bands near the conduction band edge. Here we can see an abrupt increase in the DOS at $E \cong 0.5$ eV (marked by the right arrow) which is due to the second CBM. The calculations indicate that this second band has very little dispersion in the k_z direction (perpendicular to the MS interface), which is why the increase in the DOS above ~ 0.5 eV is so strong. This is probably why this feature is observed so clearly in the derivative BEEM.

Although the derivative BEEM spectrum shows clear onsets only at $V_T \cong 1.22$ V and ~ 1.7 V, we found that we could not fit the full BEEM I_c - V_T curves very well using the BK model with two thresholds. We believe that this is because the ~ 0.5 eV energy separation of the two thresholds is so large that the BK model cannot accurately model the I_c - V_T curve for the full voltage range between the lowest threshold to the second threshold. For comparison, we note that the BK fits for the $6H$ - and $4H$ -SiC spectra shown in Figs. 2 and 4 start to show significant deviations from the data at 0.2—0.3 V above threshold. In order to determine the second threshold voltage more accurately, we adopted an approach common in other electron spectroscopies, and empirically determine a *background* spectrum (as shown by the dashed line in Fig. 7) which is smoothly varying in the vicinity of the second threshold. We then fit the Bell-Kaiser model to the difference between the data and this smooth background. The solid curve in Fig. 7 shows the sum of the smooth background and the BK fit, from which we determine the energy of the second CBM to be in the range of 0.50—0.55 eV higher than the lowest CBM.

On our $6H$ - and $4H$ -SiC samples we observed BEEM spectra and SBH's which were rather uniform over the sample. In contrast, on the $15R$ -SiC sample discussed above we observed some very interesting *spatial variations* of the BEEM spectra, as illustrated in Fig. 9. Figure 9(a) shows an example of a BEEM spectrum measured at a different sample location from that shown in Fig. 7, but showing very similar spectral features. This shows that the second CBM located ~ 0.5 eV above the first CBM is reproduced at other sample locations. However, Fig. 9(b) (which was measured at a different location) shows that certain sample locations exhibit a distinctly different spectrum. In this case, the data show a much faster rise above threshold than the data in Fig. 7 or Fig. 9(a), and show little evidence of a second CBM at higher energies. We note that data in Fig. 9(b) close to threshold can be fit well by the BK model assuming a single threshold, and in fact appears qualitatively similar to the $6H$ -SiC spectra shown in Fig. 2.

One possible origin of the observed spatial variations in BEEM spectra on this Pd/ $15R$ -SiC sample is that there might actually exist *microscopic* regions of the $6H$ -SiC polytype intermixed with $15R$ -SiC regions.¹⁹ As mentioned in Section II, the epitaxial SiC film of this particular sample was grown on a substrate that had *macroscopically separated* regions of the $15R$ and $6H$ polytypes. It is possible that there might have been some microscopic intermixing of these polytypes as well, which we are able to resolve using BEEM. Further experiments on other, more uniform $15R$ -SiC samples will help to test this possible explanation. We should also consider the possibility that such spatial variations could result from spatial variations in hot-electron transport in the metal film. As suggested by Garcia-Vidal *et al.*,¹⁷ the band structure of metal film could conceivably favor certain crystalline directions for transport of hot electrons across the metal film, and hence favor transport of BEEM electrons into CBM in the SiC which are located at specific positions in momentum space. Since the Pd metal film is polycrystalline, each Pd grain may have a different crystal orientation, and

hence different grains could favor different CBM. In this scenario, BEEM spectra as shown in Fig. 7 or Fig. 9(a) would occur if transport to the L point in the BZ were favored or comparable to transport to the X point (see Fig. 8), in which case both CBM would be observed. However, if transport to the X point were strongly favored, then the BEEM current due to the (lower energy) CBM at the X point might swamp the BEEM current to the (higher energy) CBM at L , making this higher CBM difficult to resolve. Further work needs to be done to resolve this issue.

VII. Summary

We have used BEEM to make microscopic measurements of Pd and Pt Schottky contacts on $6H$ -, $4H$ -, and $15R$ -SiC, and show that it is a valuable and versatile technique for studying spatial uniformity, hot-electron stressing effects, and conduction band structure of metal/SiC interfaces. Spatial inhomogeneities of $6H$ -, and $4H$ -SiC SBH's were shown to be smaller than the instrumental uncertainties. However, we did observe significant spatial variations in BEEM spectra on a particular Pd/ $15R$ -SiC sample, which may indicate significant spatial variations in the local SiC polytype and/or local interfacial band structures. Preliminary microscopic investigations of hot-electron-induced interface modification were performed on Pt/ $4H$ -SiC, and although observed modifications were small, we did observe instances of *enhanced* ballistic transmittance over stressed regions. The measured BEEM spectra have provided the first experimental evidence of a higher-energy CBM's in $4H$ -SiC (at ~ 0.14 eV above the lowest CBM), and in $15R$ -SiC (at ~ 0.5 eV above the lowest CBM), in agreement with our theoretical band structure calculations.

The work at the Ohio State University was supported by ONR Grant No. N00014-93-0607.

REFERENCES

- [1] *Materials for High-Temperature Semiconductor Devices*, Committee on Materials for High-Temperature Semiconductor Devices, National Academy Press, Washington, D.C., 1995.
- [2] *Diamond, SiC and Nitride Wide Bandgap Semiconductors*, edited by C. H. Carter, Jr., *et al.*, Materials Research Society, Pittsburgh, Pennsylvania, 1994.
- [3] L. M. Porter and R. F. Davis, *Mater. Sci. Eng. B* **34**, 83 (1995).
- [4] J. R. Waldrop, R. W. Grant, Y. C. Wang, and R. F. Davis, *J. Appl. Phys.* **72**, 4757 (1992).
- [5] A. L. Syrkin, A. N. Andreev, A. A. Lebedev, M. G. Rastegaeva, and V. E. Chelnokov, *J. Appl. Phys.* **78**, 5511 (1995).
- [6] W. J. Kaiser and L. D. Bell, *Phys. Rev. Lett.* **60**, 1406 (1988); L. D. Bell and W. J. Kaiser, *Phys. Rev. Lett.* **61**, 2368 (1988).
- [7] E. G. Brazel, M. A. Chin, V. Narayanamurti, D. Kapolnek, E. J. Tarsa, and S. P. DenBaars, *Appl. Phys. Lett.* **70**, 330 (1997).
- [8] H.-J. Im, B. Kaczer, J. P. Pelz, and W. J. Choyke, submitted for publication.
- [9] B. Kaczer, H.-J. Im, J. P. Pelz, J. Chen, and W. J. Choyke, to be published in *Phys. Rev. B*.
- [10] S. M. Sze, *Physics of Semiconductor Devices*, 2nd ed., Wiley-International, New York 1981.
- [11] M. Methfessel, *Phys. Rev. B* **38** 1537 (1988).
- [12] M. T. Cuberes, A. Bauer, H. J. Wen, M. Prietsch, and G. Kaindl, *J. Vac. Sci. Technol. B* **12**, 2646 (1994).
- [13] B. Kaczer, Z. Meng, and J. P. Pelz, *Phys. Rev. Lett.* **77**, 91 (1996); B. Kaczer and J. P. Pelz, *J. Vac. Sci. Technol. B* **14**, 2864 (1996).
- [14] R. Ludeke, A. Bauer, and E. Cartier, *Appl. Phys. Lett.* **66**, 730 (1995).

- [15] S. Limpijumnong and W. R. L. Lambrecht, submitted for publication; W. R. L. Lambrecht, S. Limpijumnong, S. N. Rashkeev, B. Segall, *Phys. Stat. Solidi (b)* **202**, 5 (1997).
- [16] L. J. Brillson, *Surf. Sci. Rep.* **2**, 123 (1982).
- [17] F. J. Garcia-Vidal, P. L. de Andres, and F. Flores, *Phys. Rev. Lett.* **76**, 807 (1996).
- [18] H. D. Hallen, A. Fernandez, T. Huang, R. A. Buhrman, and J. Silcox, *J. Vac. Sci. Technol.* **B 9**, 585 (1991).
- [19] L. Muehlhoff, W. J. Choyke, M. J. Bozack, and J. T. Yates, Jr., *J. Appl. Phys.* **60**, 2842 (1986).

FIGURES

Fig. 1: (a) Physical setup of the BEEM experiment on SiC and (b) the corresponding energy level diagram, with the two lowest conduction band minima labeled CBM_1 and CBM_2 . By measuring the dependence of I_c (current of *ballistic* electrons from the STM tip into the SiC substrate) on tunnel voltage V_T (at constant tunnel current I_T) the local SBH and conduction band structure can be probed.

Fig. 2: Representative BEEM I_c - V_T data from metal/6H-SiC contacts made with (a) Pt and (b) Pd. Each set of data represents average of 125—175 individual BEEM I_c - V_T curves taken at different sample locations. Data in (a) are vertically offset and multiplied by a factor of 2 for clarity. Solid curves are fits to the data using (BK) model. Arrows designate thresholds extracted from the fits (see text). Inset: derivative spectrum dI_c/dV_T vs. V_T .

Fig. 3: Measured BEEM threshold voltage V_{th} vs. reverse substrate bias V_b for Pd/6H-SiC Schottky contact, showing image force lowering effect and quality of BEEM data for large reverse substrate bias. Each data point is fitted threshold voltage from an average of 25 BEEM I_c - V_T curves taken at a fixed substrate bias V_b . Estimated fitting error for each data point is ~ 5 meV. Solid curve is a least square fit to the obtained data using the image-force-lowering model from Ref. 10, assuming SiC specific dielectric constant $\epsilon = 9.8$ and donor density $N_D = 3 \times 10^{16} \text{ cm}^{-3}$. Inset shows a schematic diagram of effective barrier lowering as the reverse bias increases ($V_{bl} > V_{b2}$).

Fig. 4: Representative BEEM I_c - V_T data from metal/4H-SiC contacts made with (a) Pt and (b) Pd. Each set of data represents average of 150—175 individual BEEM I_c - V_T curves taken at different sample locations. Data in (a) are vertically offset and multiplied by a factor of 2 for clarity. Solid curves are fits to the data using the BK model with two independent thresholds for each curve. Arrows designate thresholds extracted from the fits (see text). Inset: derivative spectrum dI_c/dV_T vs. V_T , showing distinct slope increase, indicating onset of a higher energy CBM.

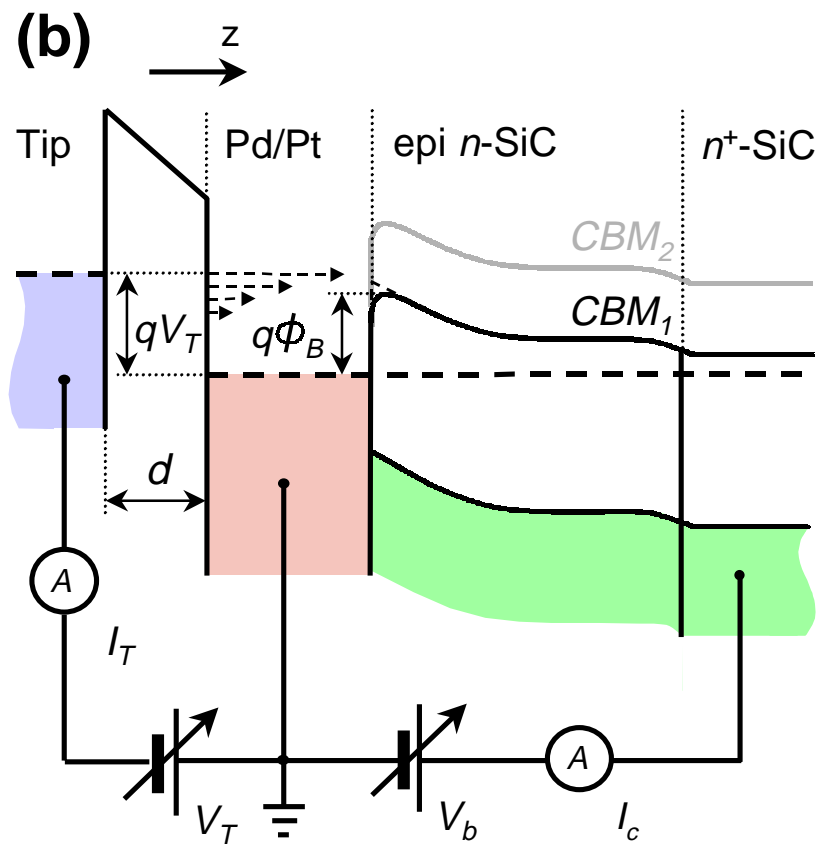
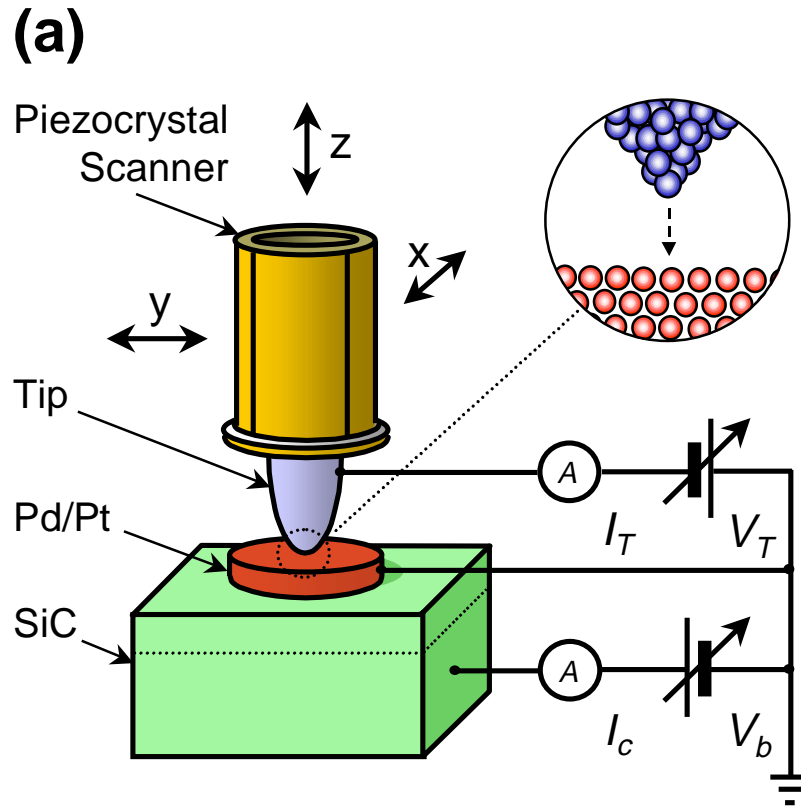
Fig. 5: Calculated total conduction band DOS (solid curves) for (a) $6H$ and (b) $4H$ polytypes of SiC, with energy referenced to the lowest CBM. Arrows mark abrupt increase in DOS due to CBM's (see text). The $4H$ -SiC DOS plot in (b) shows a distinct increase at ~ 0.12 eV (marked by the right arrow) due to a higher-energy CBM.

Fig. 6: (a) 150×150 nm² topographic image and (b) corresponding BEEM image of 6 nm-Pt/ $4H$ -SiC contact, measured with $V_T = 2$ V and $I_T = 10$ nA. Grey-scale range is ~ 5 nm for (a) and ~ 2 pA for (b). A 40-minute “stressing” scan with $V_T = 10$ V and $I_T = 10$ nA was then done over region outlined by dashed boxes. (c) and (d) show “post-stress” topography and BEEM image, respectively, and indicate slightly enhanced BEEM current in stressed region (solid boxes).

Fig. 7: BEEM I_c - V_T data (circles) for 6 nm-Pd/ $15R$ -SiC taken at a particular location. Over 100 BEEM spectra at the same location were averaged to improve signal-to-noise. Dashed curve is smooth empirical background, while solid curve is fit of data to BK model with additional threshold near ~ 1.75 V (see text). Inset: derivative spectrum dI_c/dV_T vs. V_T , showing distinct slope increase at ~ 1.75 V, indicating onset of a higher energy CBM.

Fig. 8: (a) Two lowest calculated conduction bands for $15R$ -SiC, with CBM's located at X -point ($E = 0$) and L -point ($E = \sim 0.5$ eV), respectively. Inset: BZ for $15R$ -SiC, with a few symmetry points labeled. (b) Calculated total DOS (solid curve) for $15R$ -SiC near the conduction band edge. There is an abrupt increase in DOS at $E = \sim 0.5$ eV (marked by the right arrow) due to the higher-energy CBM at the L -point (see text).

Fig. 9: BEEM I_c - V_T data (circles) and a BK fits (solid curves) for 6 nm-Pd/ $15R$ -SiC taken at two different locations from the data in Fig. 7. Each curve represents average of over 100 individual I_c - V_T curves measured at the same location. (a) BEEM spectrum which appears very similar to Fig. 7, indicating this type of spectrum is commonly seen over the surface. (b) BEEM spectrum at different location with a distinctly different shape. Insets: derivative spectra dI_c/dV_T vs. V_T for the two cases, showing distinctly different features. Inset in (a) shows clear indication of a CBM at ~ 0.5 eV above the first, while inset in (b) shows little indication of second CBM.



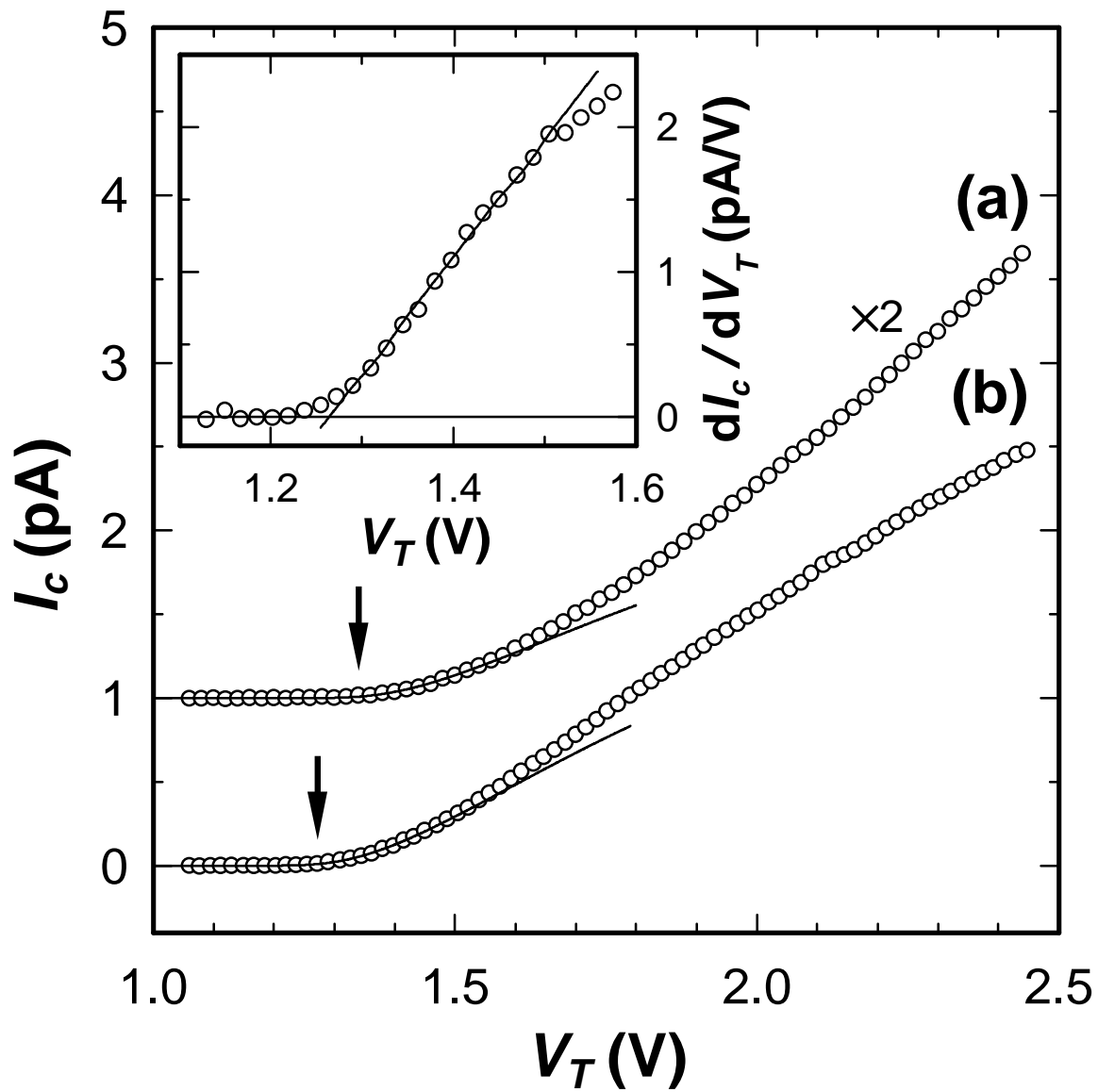


Fig. 2/9

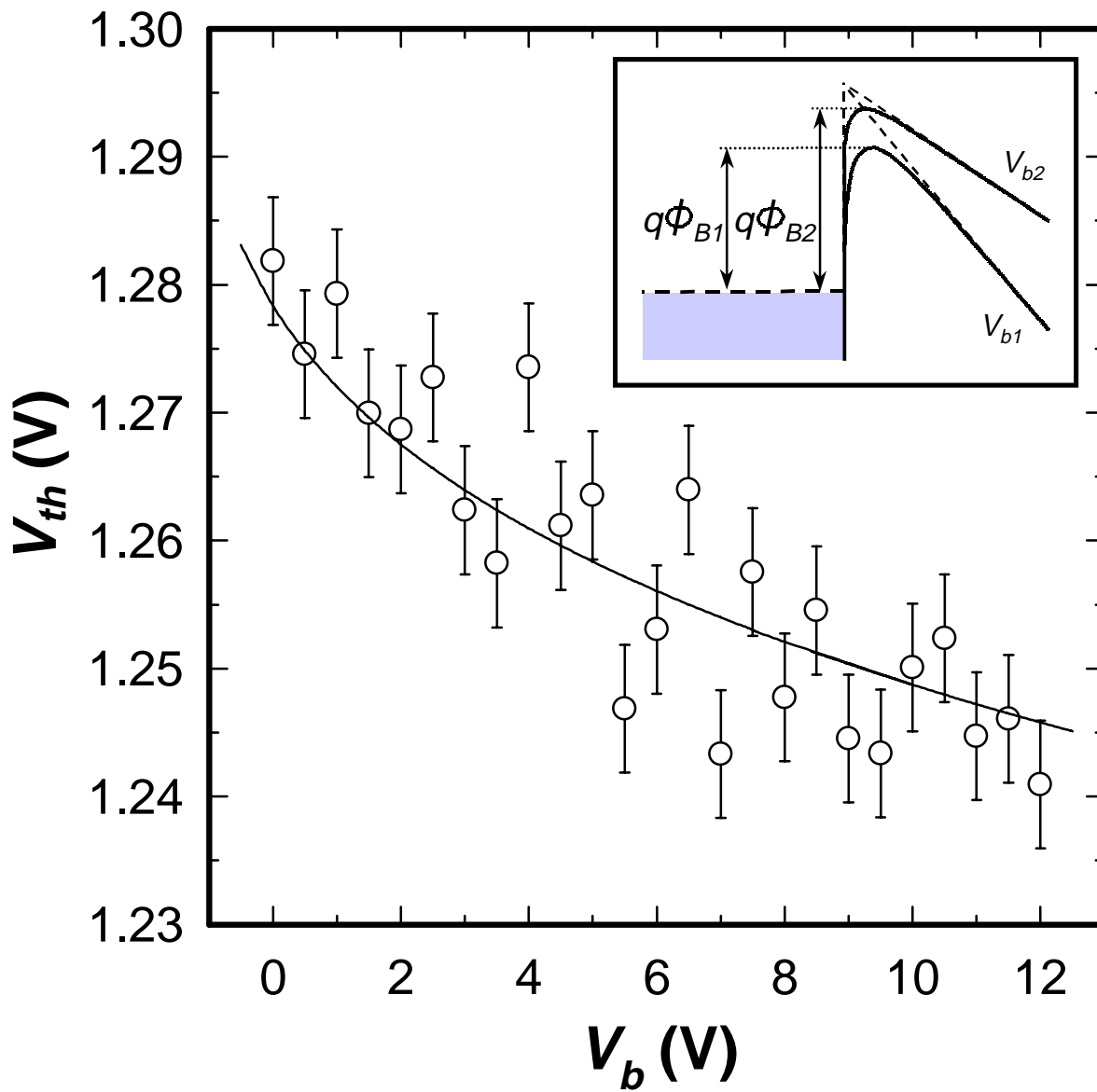


Fig. 3/9

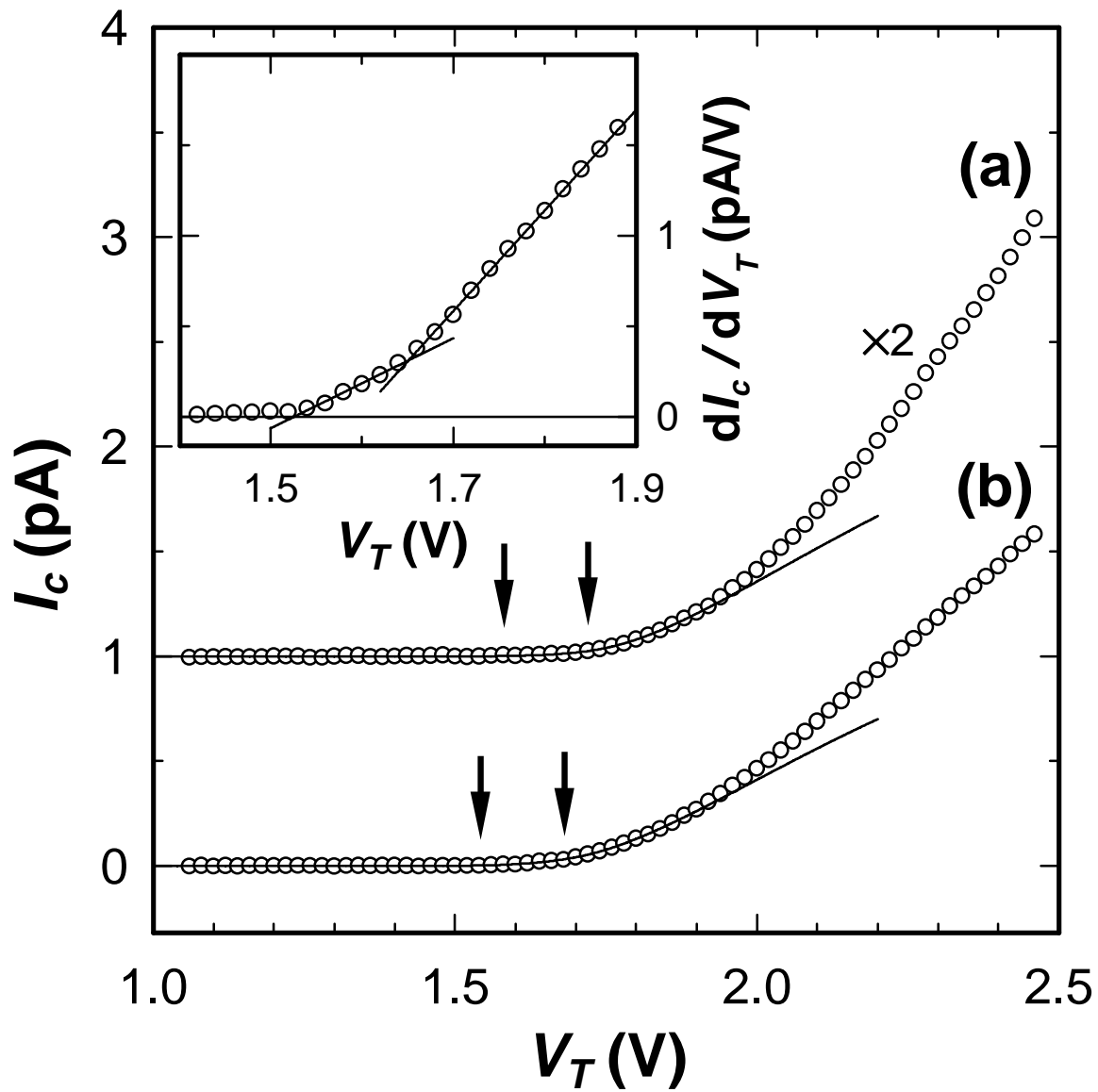


Fig. 4/9

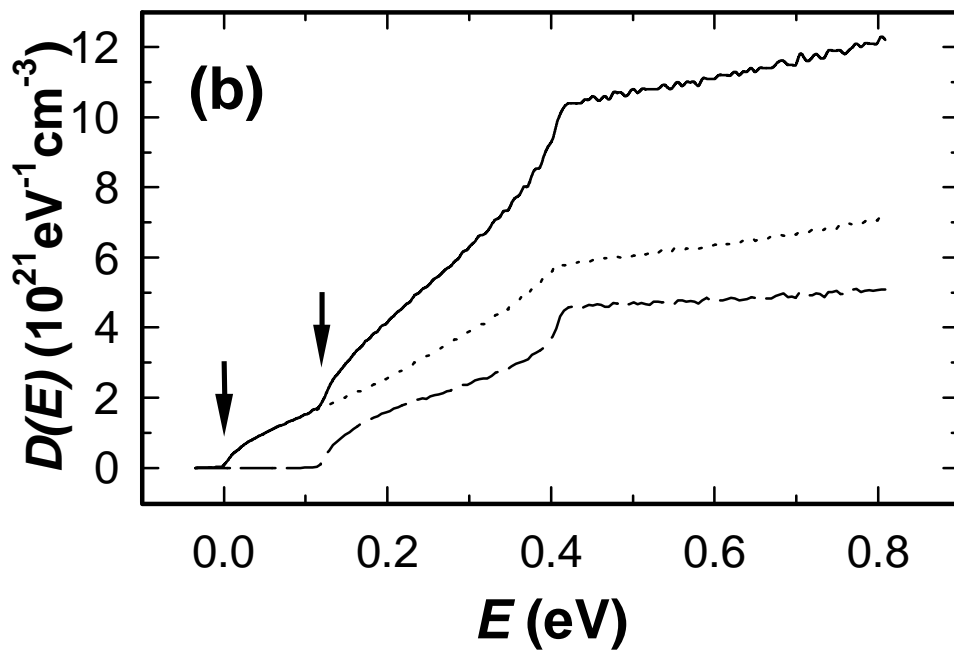
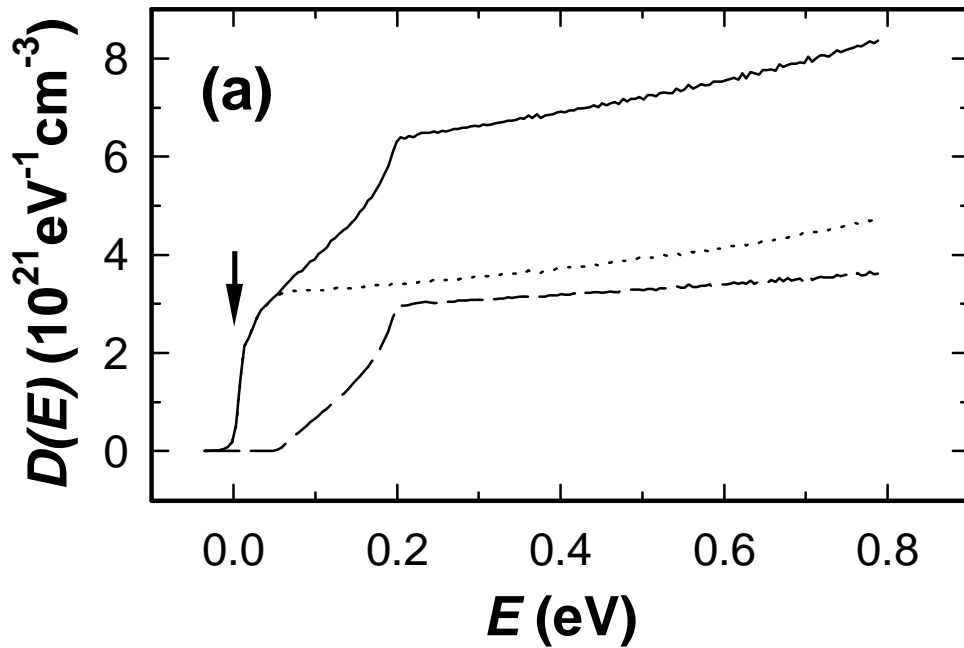


Fig. 5/9

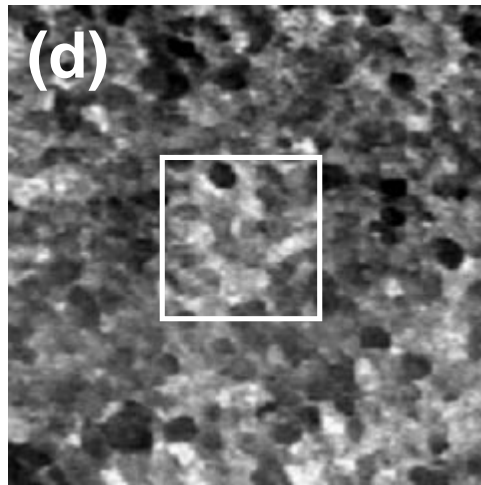
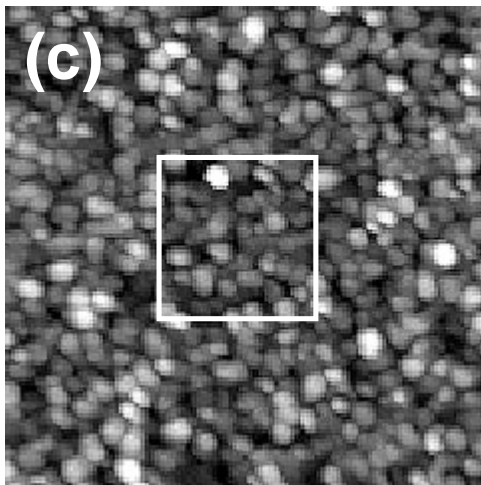
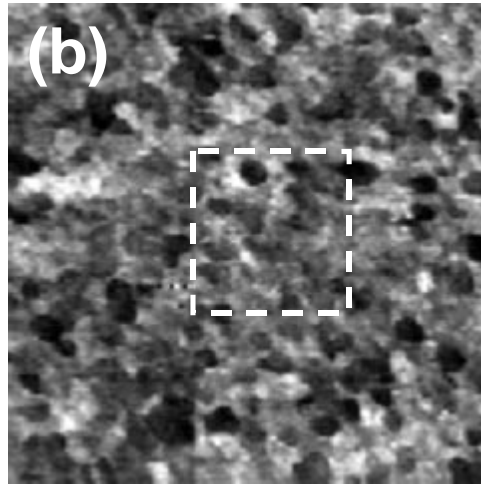
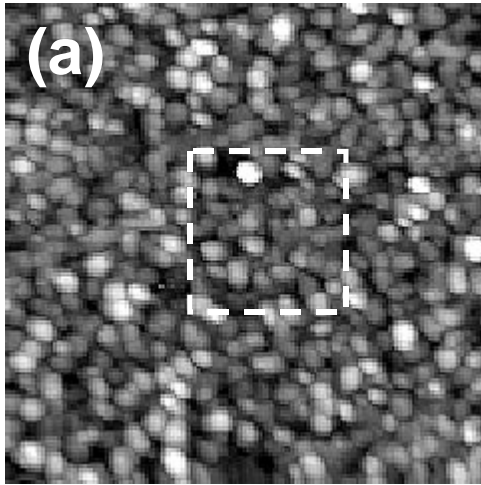


Fig. 6/9

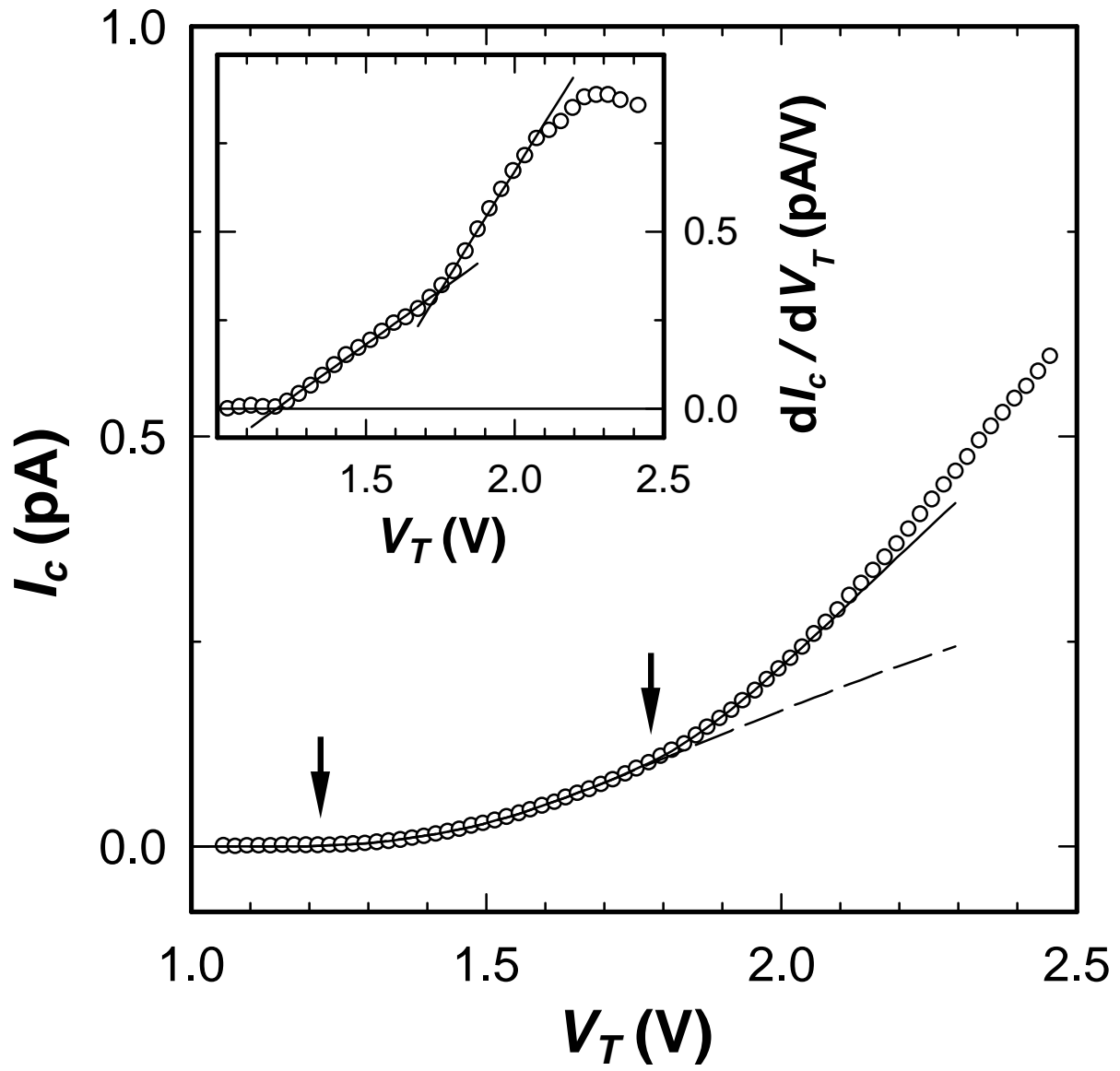


Fig. 7/9

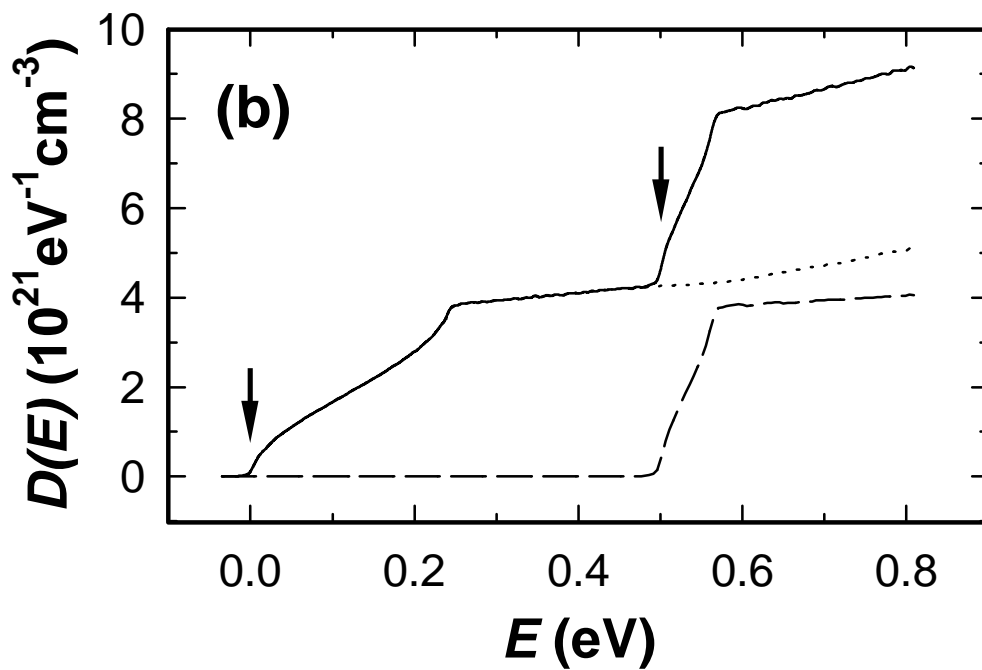
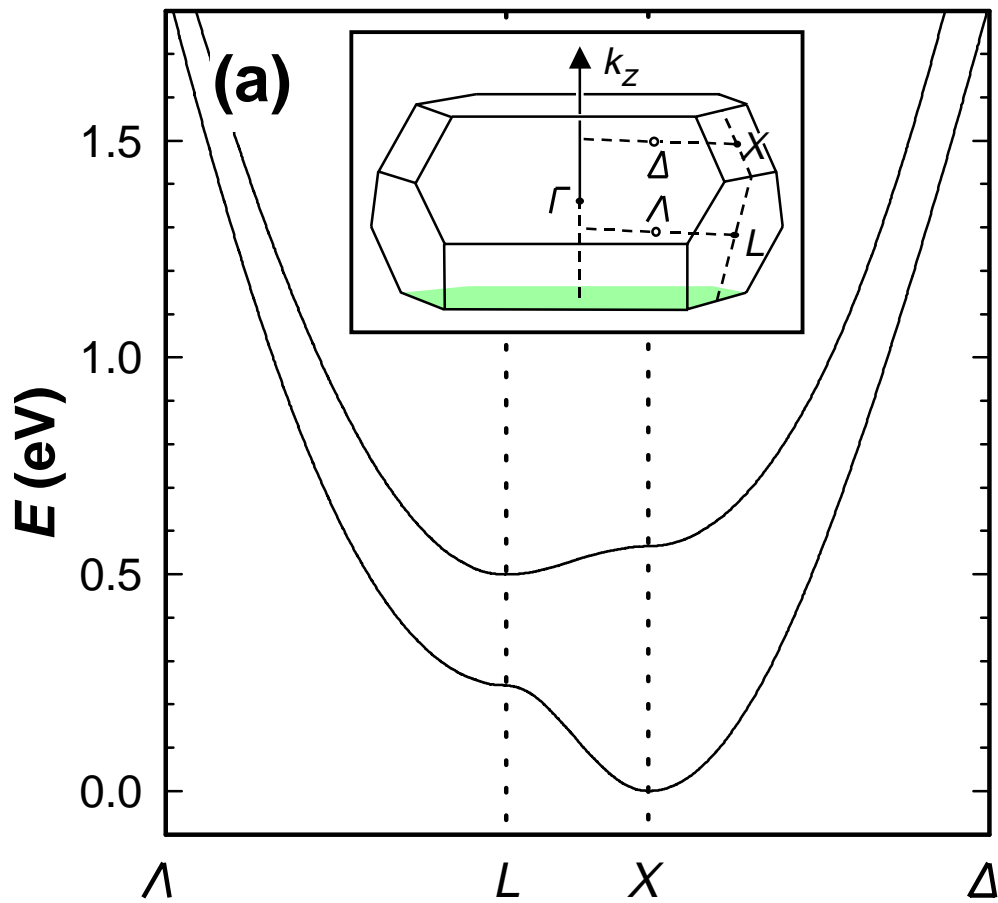


Fig. 8/9

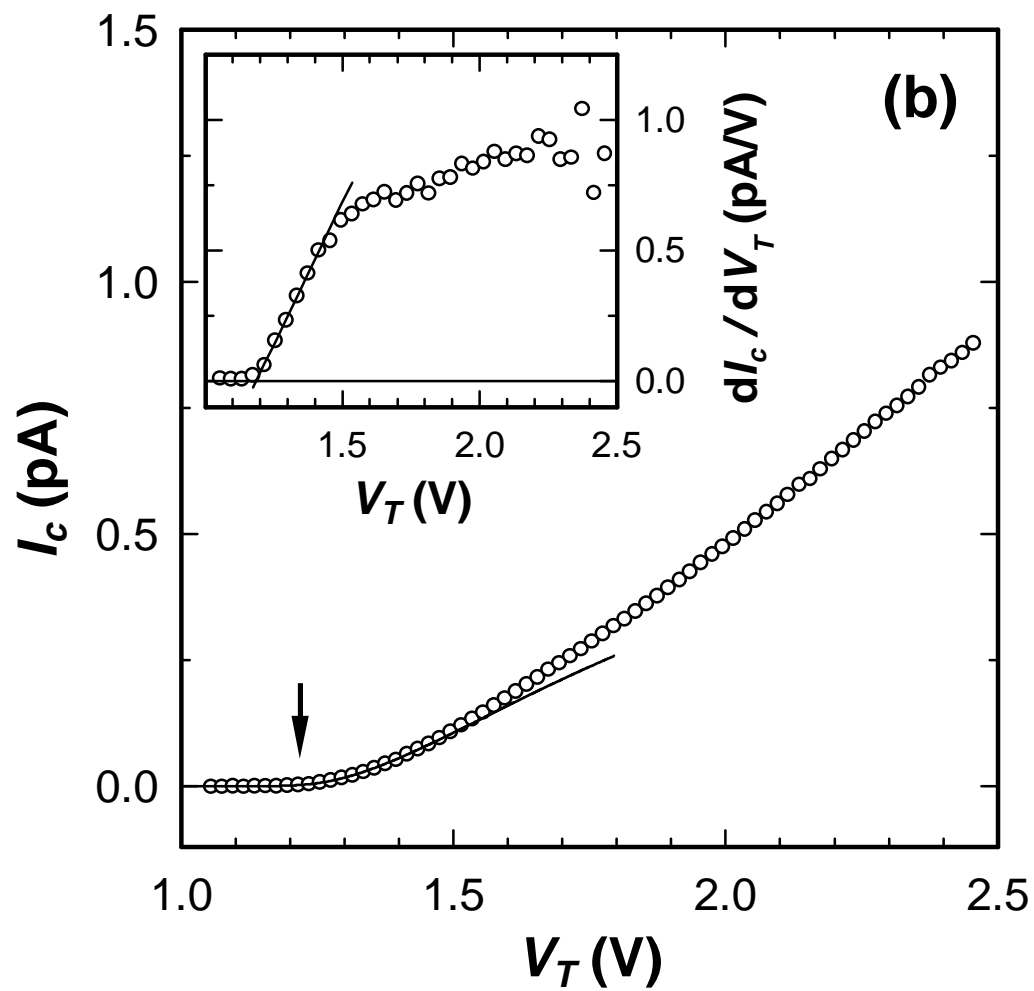
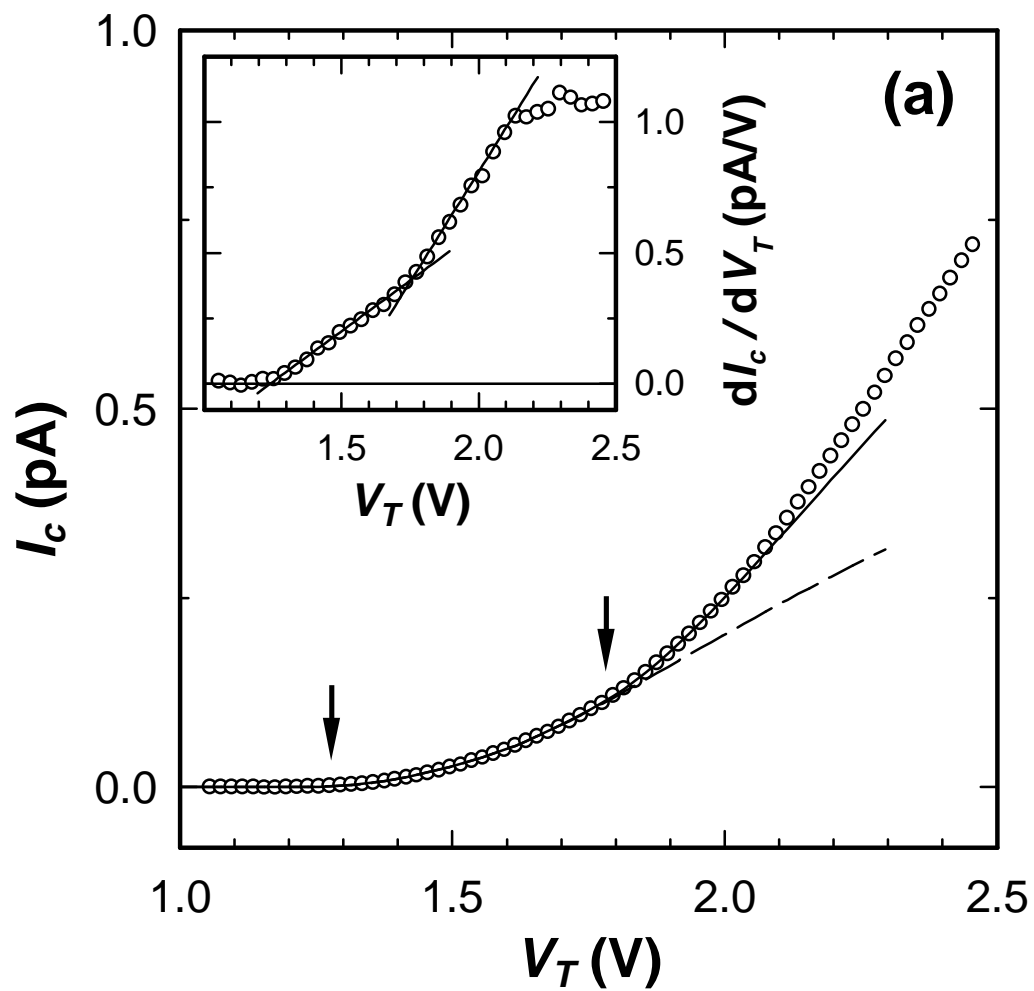


Fig. 9/9